Supplementary Information (SI) for Physical Chemistry Chemical Physics.

Electronic Supplementary Information: Kinetics of Radiation-Induced Cr(II) and Cr(III) Redox Chemistry in Molten LiCl-KCl Eutectic

Kazuhiro Iwamatsu,* Gregory P. Horne,* Alejandro Ramos-Ballesteros, Stephanie Castro Baldivieso, Jacy K. Conrad, Michael E. Woods, William C. Phillips, Jay A. LaVerne, Simon M. Pimblott, and James F. Wishart*

Additional Transient Absorption Spectra

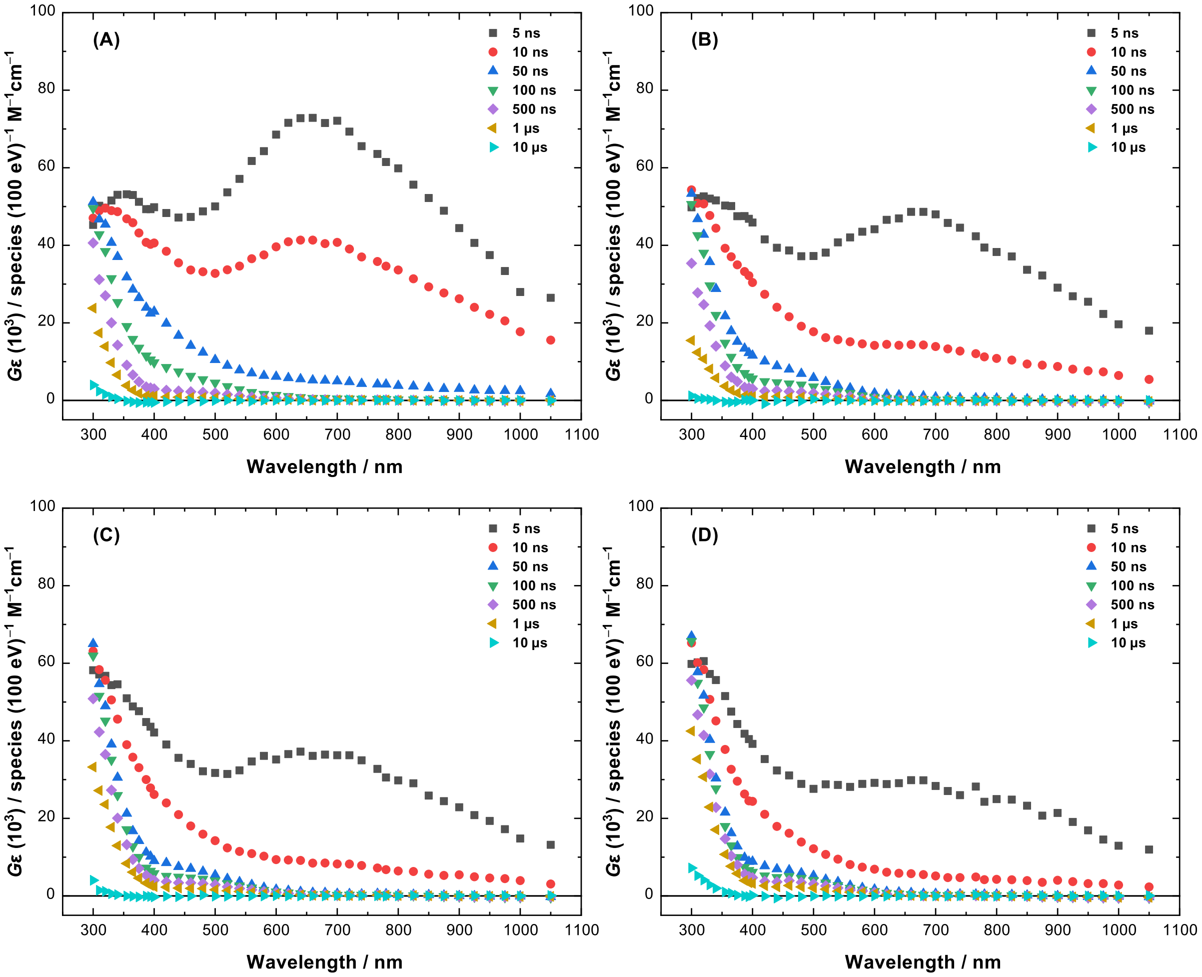

Fig. S1. Transient absorption spectra at selected times for different concentrations of $CrCl_2$ in LiCl-KCl eutectic at 400 °C: 0.99 **(A)**, 3.10 **(B)**, 4.03 **(C)**, and 4.99 **(D)** mM.

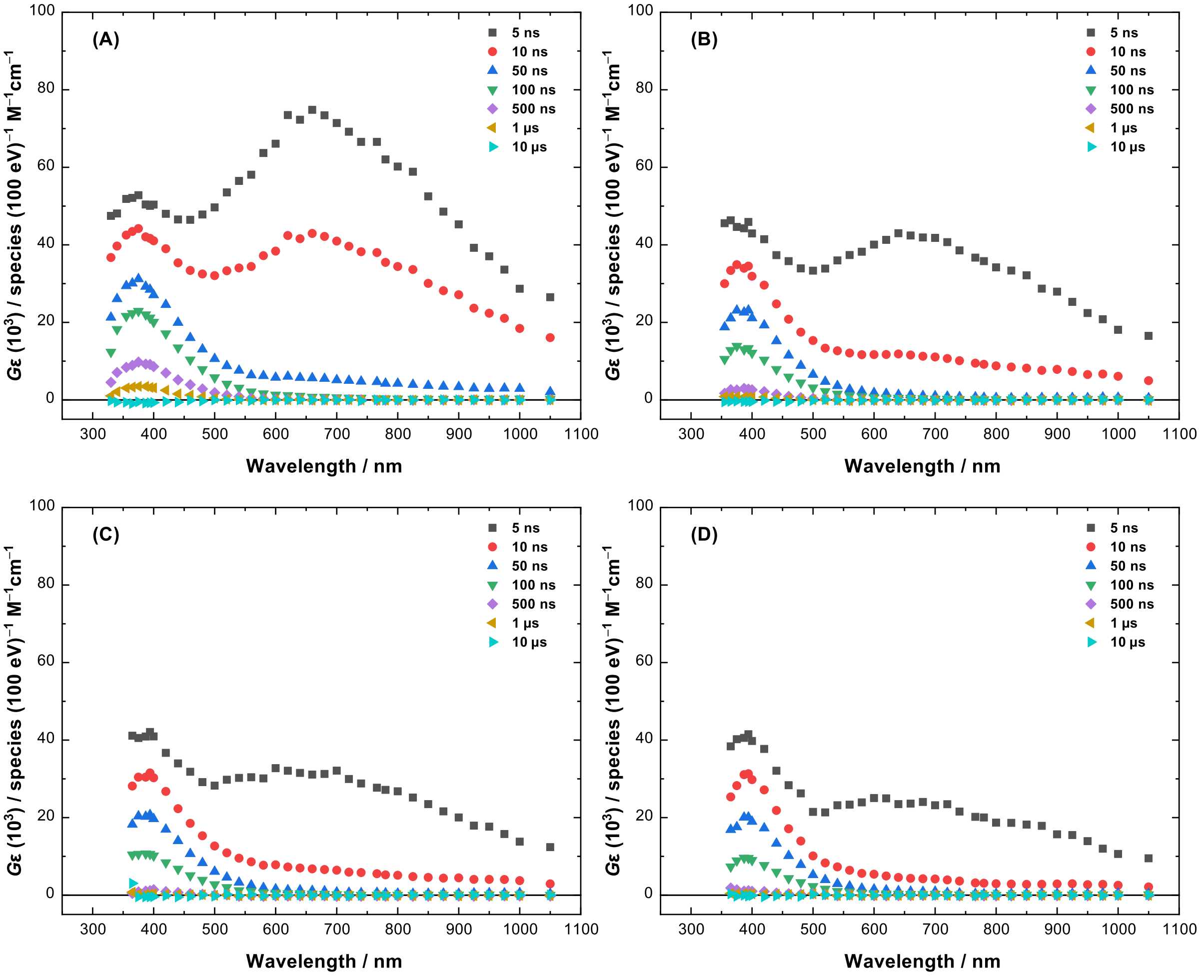

Fig. S2. Transient absorption spectra at selected times for different concentrations of $CrCl_3$ in LiCl-KCl at 400 °C: 1.00 **(A)**, 2.98 **(B)**, 3.91 **(C)**, and 4.97 **(D)** mM.

Activation Energy Plots

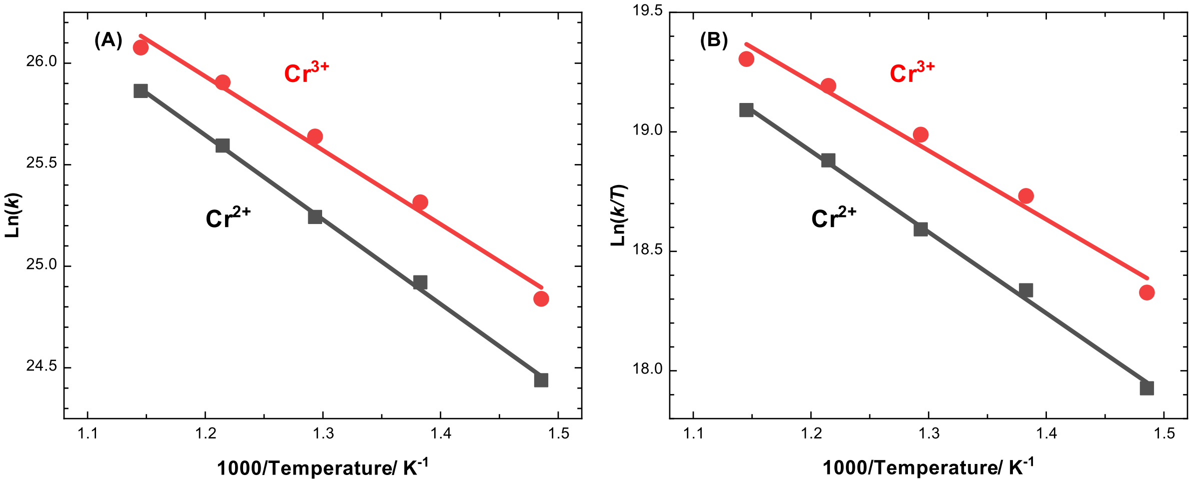

Fig. S3. Arrhenius **(A)** and Eyring **(B)** plots for reaction of e_S^- with Cr(II) (**black**) or Cr(III) (**red**) using measured rate coefficient at temperature from 400 to 600 °C.

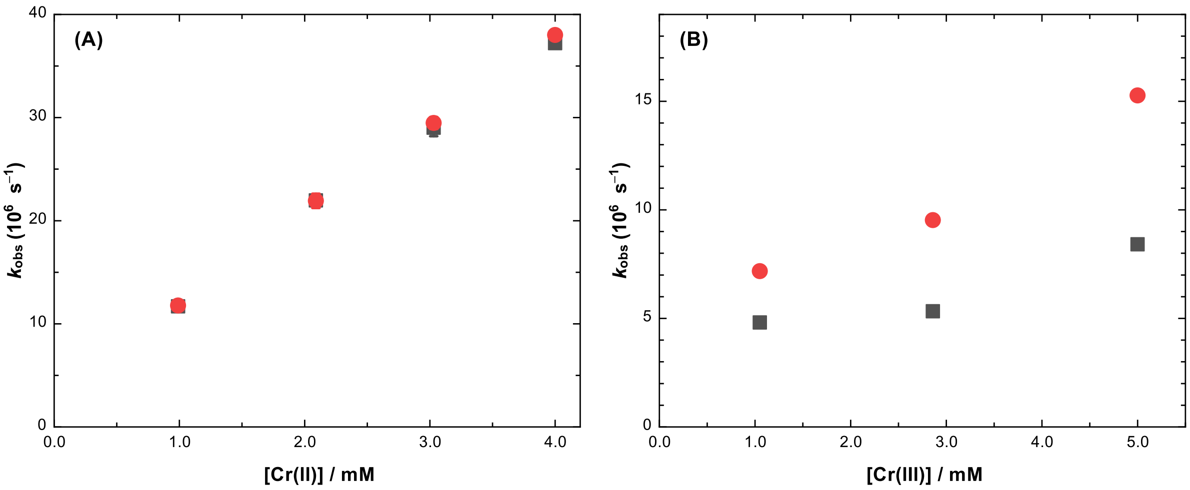

Fig. S4. Observed pseudo-first-order rate coefficients for **Eq. 9 (A)** and **Eq. 10 (B)** at 400 nm as a function of CrCl$_2$ and CrCl$_3$ concentration, respectively, for low (200–600 Gy, ■) and high (up to 3000 Gy, ●) cumulative electron dose. Error bars are one standard deviation using four repeated measurements at each experimental condition. (They are smaller than the symbols.)

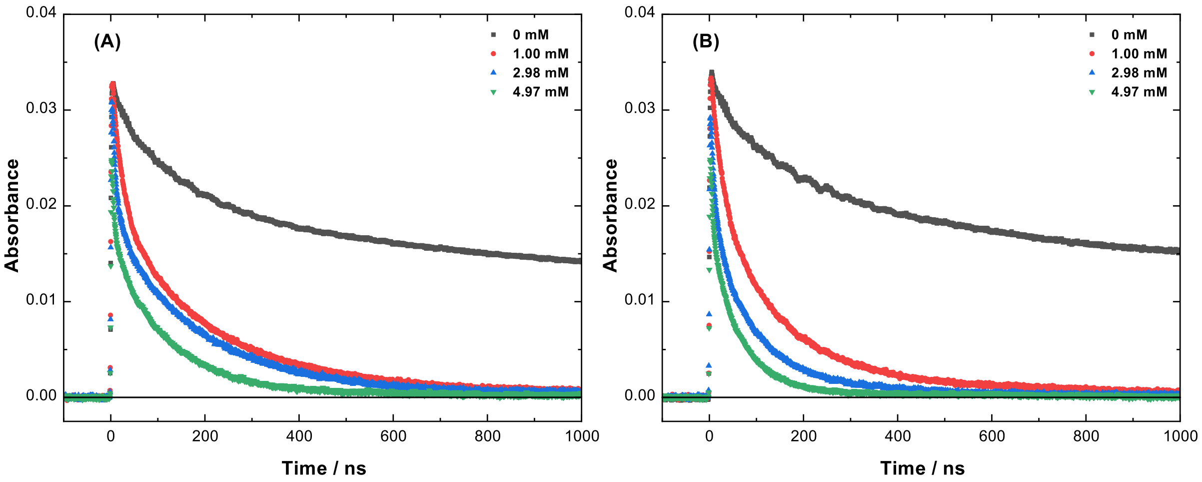

Fig. S5. Transient absorption kinetics at 400 nm as a function of CrCl$_3$ concentration: 0 (**black**), 1.05 (**red**), 2.98 (**blue**) and 4.97 (**green**) at 400 °C for low (200–600 Gy, **A**) and high (up to 3000 Gy, **B**) cumulative electron dose.

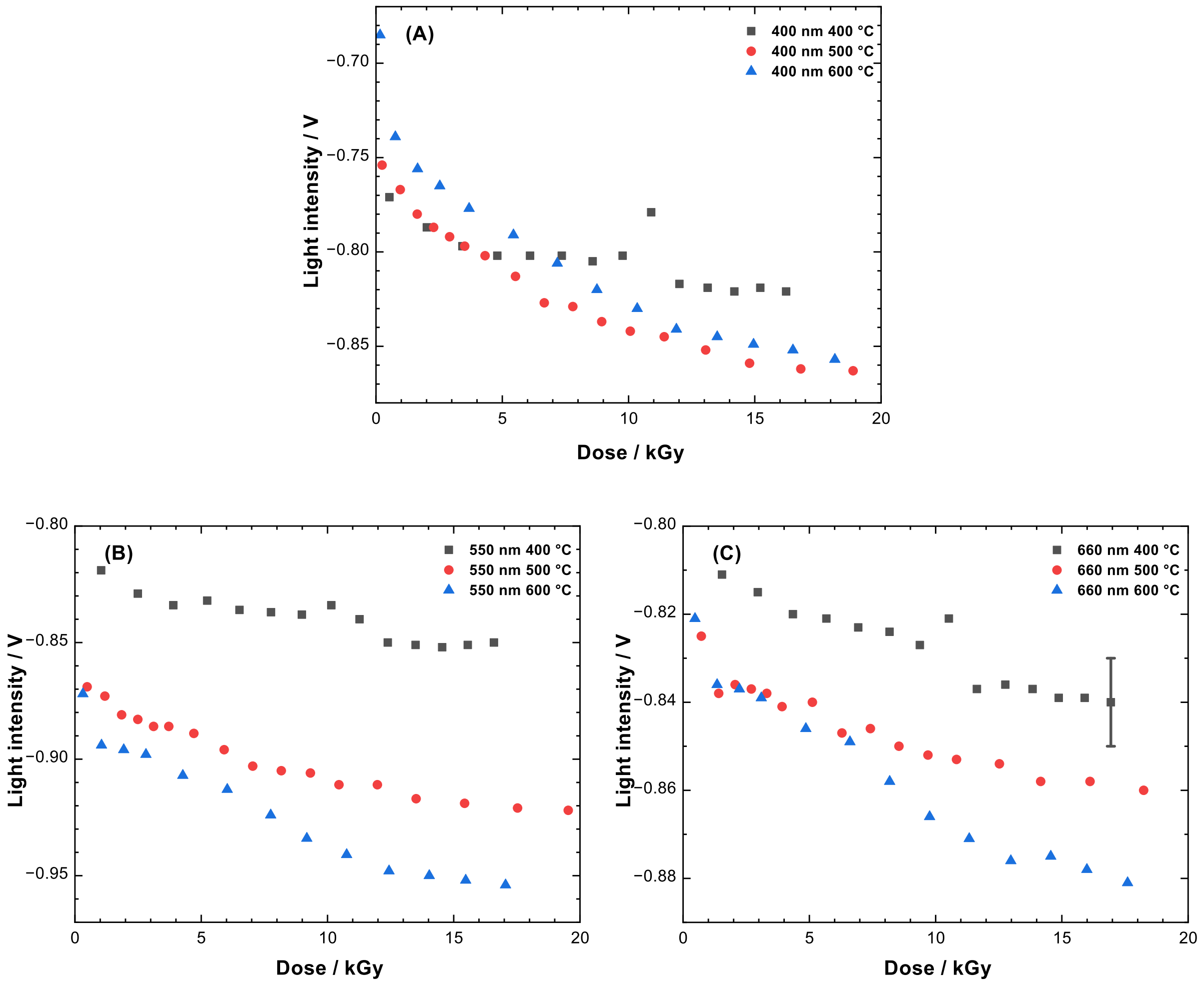

Fig. S6. Analysing light intensity as a function of cumulative electron dose in 2.11 mM $CrCl_3$ in LiCl-KCl at 400 **(A)**, 550 **(B)** and 660 **(C)** nm for 400 (■), 500 (●), and 600 (▲) °C. The error bar shown on the last point of 660 nm at 400 °C in **(C)** is a generous estimate of the uncertainty due to light intensity drift for the measurement period (~one hour). It was estimated using light intensity data from repeated measurements with aqueous solutions at 650 nm under the same experimental set up.

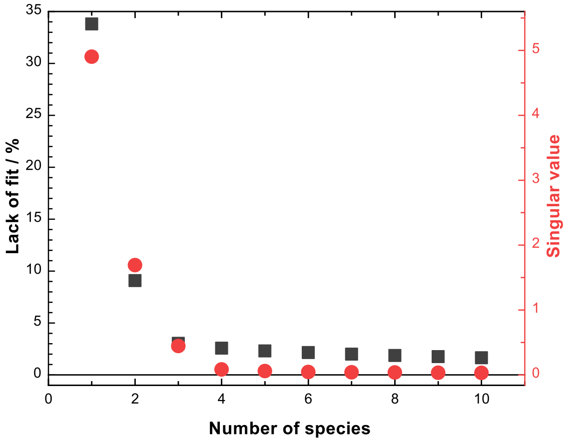

Fig. S7. Lack of fit values (**black**) and singular values (**red**) of multiple components obtained using SK-Ana deconvolution of the measured absorbance vs. time and wavelength transient data matrix for 2.01 mM $CrCl_2$ in LiCl-KCl eutectic at 400 °C.

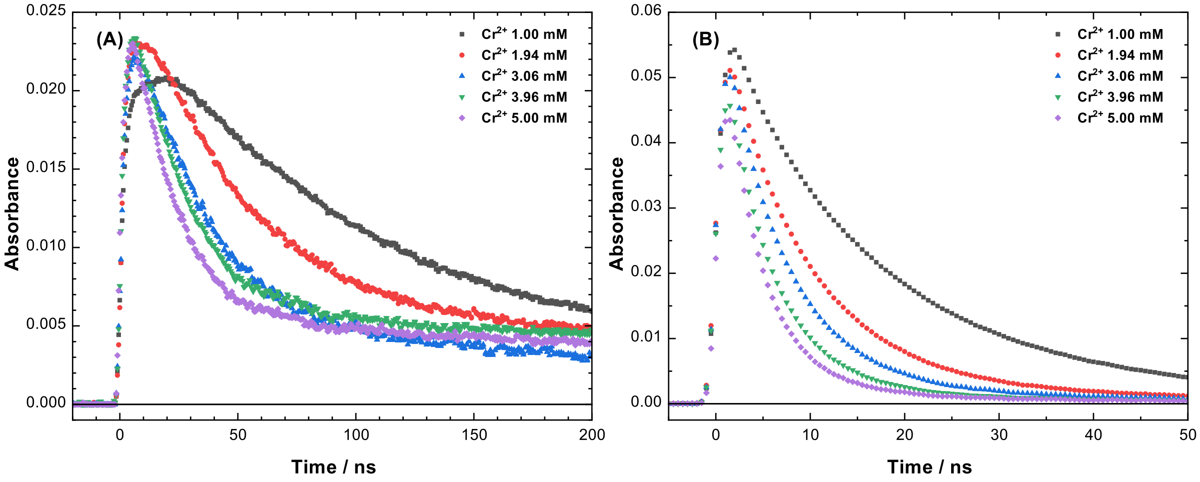

Fig. S8. Kinetics traces derived by SK-Ana for species S1 **(A)** and S2 **(B)** assigned as $Cl_2^{\bullet -}$ and e_S^-, respectively, at each maximum wavelength for different $CrCl_2$ concentrations.

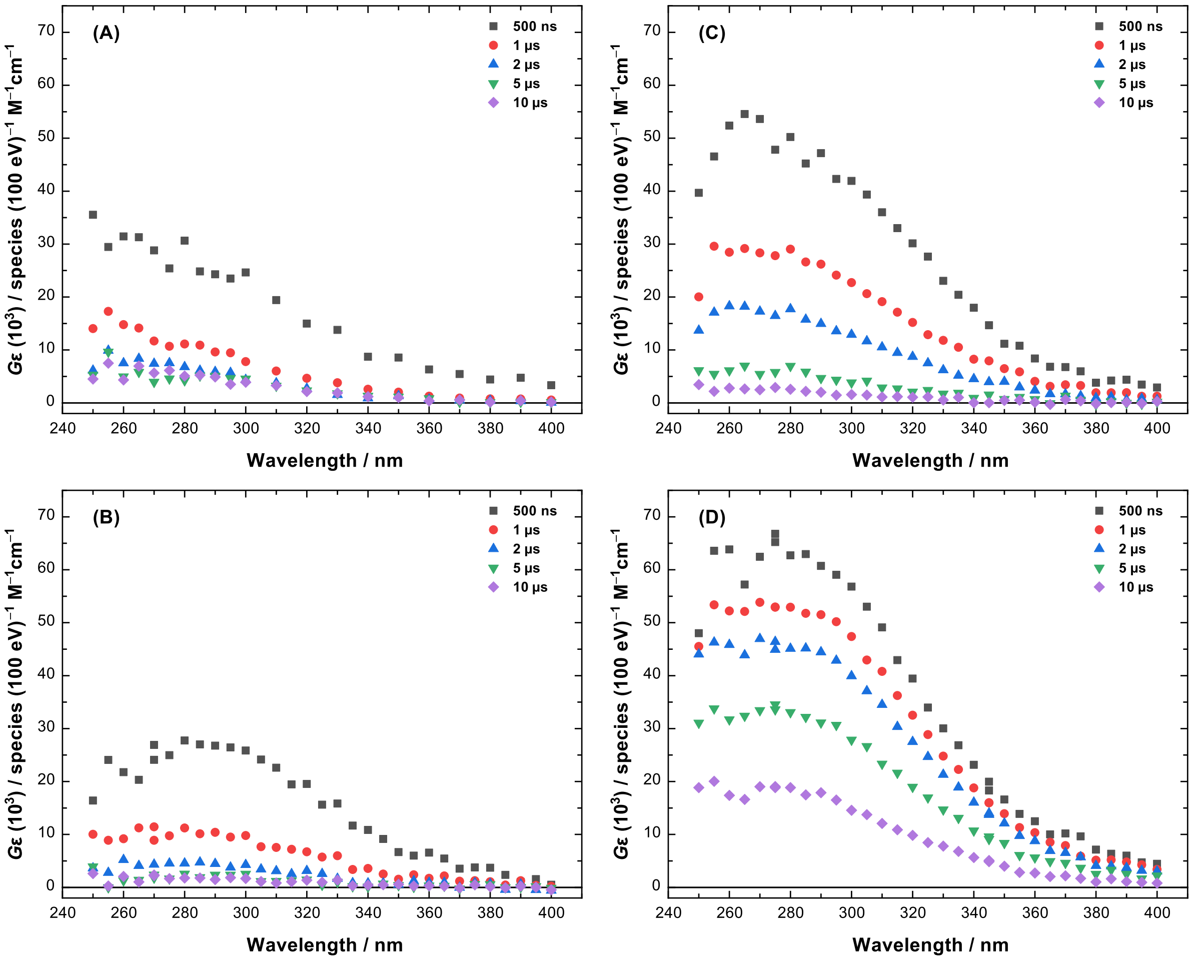

Fig. S9. Transient absorption spectra at selected times for different concentrations of $CrCl_2$ in LiCl-KCl eutectic at 400 °C, measured further into the UV using the 2 MeV VdG detection system: **(A)** 0.99 mM, **(B)** 3.10 mM, **(C)** 4.99 mM, and **(D)** 8.72 mM. The data in Figs. S9D and 7A, using the same concentration were collected at different

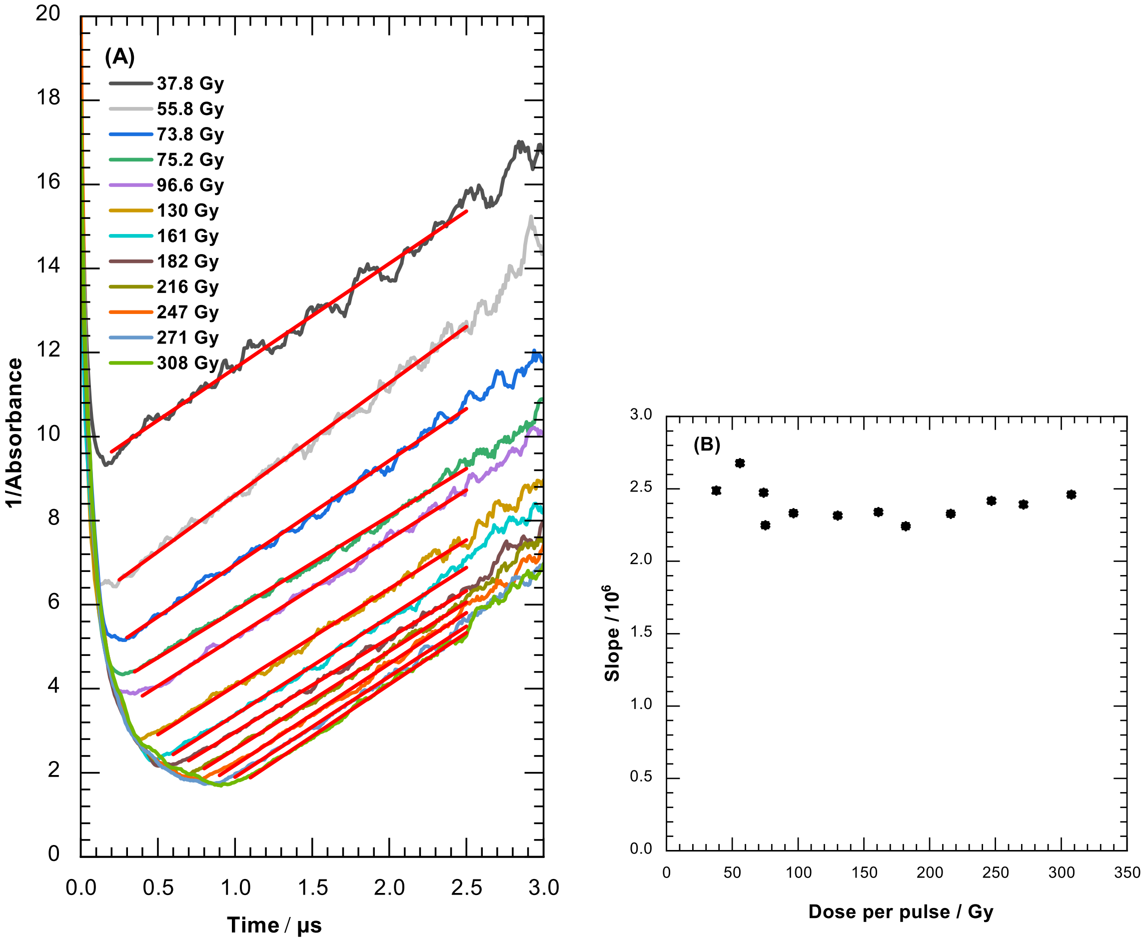

Fig. S10. (A) Inverse absorbance plot of the data presented in **Fig. 7B** for 8.72 mM $CrCl_2$ in LiCl-KCl eutectic at 400 °C, over a dose range of 39–333 Gy. Linear fits to the data at each dose are indicated over the fitted range. Pathlength 0.5 cm. (**B)** Slopes obtained from the linear fits in part (A) plotted as a function of dose. Error bars are shown at one standard deviation for all points within fitting range. (They are usually smaller than the symbols.)

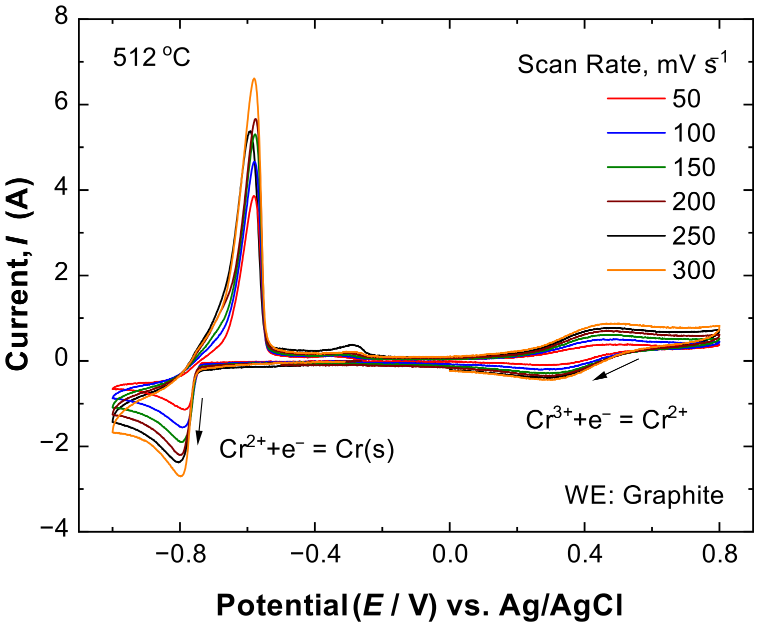

Fig. S11. Cyclic voltammograms of 15 mM $CrCl_2$ in eutectic LiCl-KCl at 510 °C, recorded at scan rates from 50–300 mV s^{-1} using a graphite working electrode (surface area: 0.228 cm^2) and an Ag/AgCl reference electrode. The voltammograms are not IR corrected.

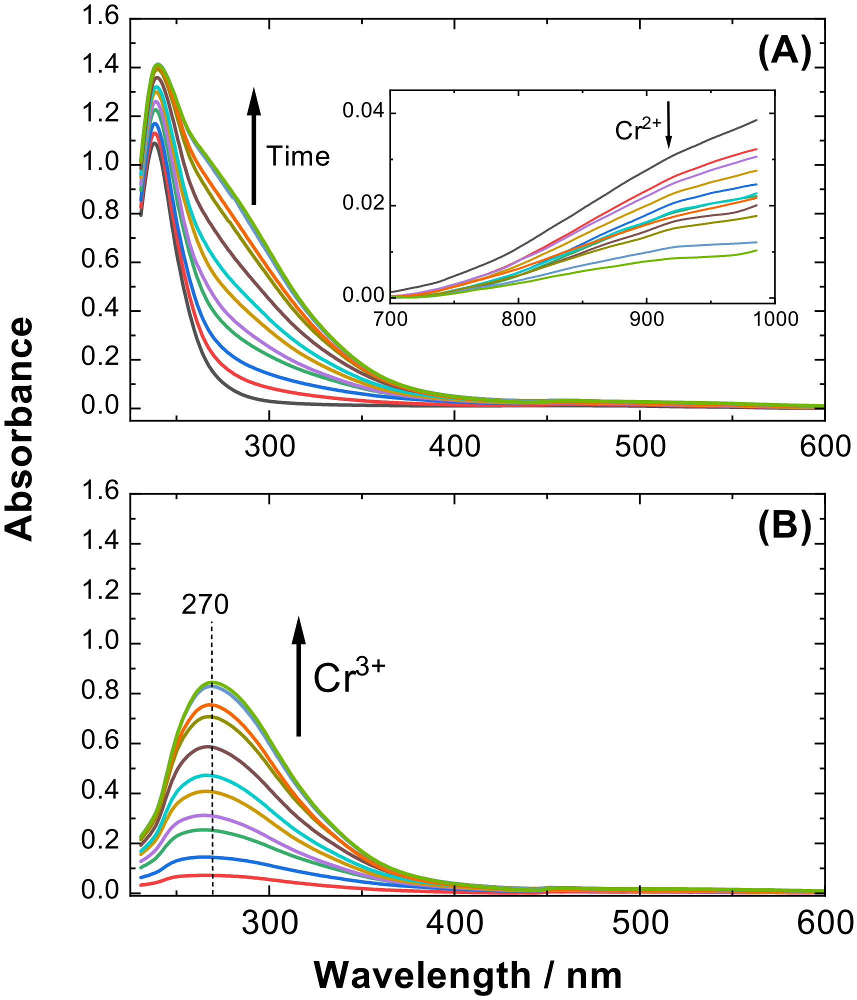

Fig. S12 (A) UV-Vis spectra of the chronoamperometric oxidation of 4 mM $CrCl_2$ in eutectic LiCl-KCl at 510 °C and a fixed potential of +0.500 V vs. Ag/AgCl. Starting from the bottom trace, spectra were recorded at 10-minute intervals. Inset: Expansion of NIR region showing consumption of Cr(II) with time. (**B)** Cumulative difference spectra showing increasing absorbance due to Cr(III) as the electrolysis continued. Each difference spectrum was calculated from the data in **part A** above by subtracting the bottom trace from the corresponding measured absorbance trace of the same colour. At longer times, the difference absorbance values below 250 nm may be suppressed due to saturation of the dynamic range of the spectrometer.

Electron Density Dose Correction Values

Table S1. Summary of density values for molten LiCl-KCl eutectic at each temperature investigated by this study, and the associated electron density ratios vs. water at room temperature.

Temperature (°C)	Density of salt (g cm^{-3})*	Electron density ratio vs. water
400	1.677	1.444
450	1.651	1.422
500	1.625	1.399
550	1.599	1.376
600	1.573	1.355

* G.J. Janz, F.W. Dampier, G.R. Lakshminarayanan, P.K. Lorenz, R.P.T. Tomkins, *Molten Salts: Volume 1, Electrical Conductance, Density, and Viscosity Data*, U.S. Department of Commerce/National Bureau of Standards, NSRDS-NBS61, Part II, 1979.

Observed Pseudo-First-Order and Calculated Second-Order Rate Coefficients

Table S2. Average observed pseudo-first-order and calculated second-order rate coefficients for the reactions of the e_s^- with Cr(II) and Cr(III) ions in molten LiCl-KCl eutectic.

Temperature / °C	400	450	500	550	600	400
Cr(II)						
$[Cr^{2+}]$ / mM	0.99	0.98	0.96	0.94	0.93	0.99
k_{obs} / 10^8 s^{-1}	0.62	1.00	1.44	1.86	2.34	0.62
$[Cr^{2+}]$, mM	2.09	2.06	2.03	1.99	1.96	2.09
k_{obs}, x 10^8 s^{-1}	0.98	1.56	2.21	3.03	3.81	1.00
$[Cr^{2+}]$, mM	3.03	2.99	2.94	2.89	2.85	3.03
k_{obs}, x 10^8 s^{-1}	1.38	2.13	2.87	4.23	5.41	1.35
$[Cr^{2+}]$, mM	4.00	3.94	3.88	3.82	3.76	4.00
k_{obs}, x 10^8 s^{-1}	1.76	2.83	3.88	5.22	6.70	1.88
k_5, x 10^{10} M^{-1} s^{-1}	4.1 ± 0.2	6.7 ± 0.4	9.2 ± 0.6	13.0 ± 0.7	17.1 ± 0.9	4.6 ± 0.3
Cr(III)						
$[Cr^{3+}]$ / mM	1.05	1.04	1.02	1.00	0.99	1.05
k_{obs} / 10^8 s^{-1}	0.60	0.91	1.35	1.89	2.23	0.52
$[Cr^{3+}]$ / mM	2.02	1.98	1.95	1.92	1.89	2.02
k_{obs} / 10^8 s^{-1}	1.23	2.03	2.87	3.80	4.18	1.07
$[Cr^{3+}]$ / mM	2.86	2.81	2.77	2.72	2.68	2.86
k_{obs} / 10^8 s^{-1}	1.75	2.96	3.91	5.49	5.79	1.50
$[Cr^{3+}]$ / mM	3.81	3.75	3.69	3.63	3.57	3.81
k_{obs} / 10^8 s^{-1}	2.59	4.15	5.54	7.11	8.84	2.21
$[Cr^{3+}]$ / mM	5.00	4.92	4.84	4.77	4.69	5.00
k_{obs} / 10^8 s^{-1}	2.98	4.63	6.46	8.32	9.49	2.69
k_6 / 10^{10} M^{-1} s^{-1}	6.1 ± 0.3	9.9 ± 0.7	13.6 ± 0.6	17.8 ± 0.9	21.1 ± 1.6	5.6 ± 0.3

Table S3. Average observed pseudo-first-order rate coefficients at 400 °C for the reactions of $Cl_2^{\bullet-}$ with Cr(II) in molten eutectic LiCl-KCl at the indicated concentrations.

[Cr^{2+}] (mM)	**k_{obs} (10^7 s^{-1})**
0.99	1.01
2.01	1.90
3.01	2.42
4.03	3.20
4.99	3.99

Table S4. Average observed pseudo-first-order rate coefficients at 400 °C for the reactions of $Cl_2^{\bullet-}$ with Cr(III) in molten eutectic LiCl-KCl at the indicated concentrations.

[Cr^{3+}] (mM)	**k_{obs} (10^7 s^{-1})**
1.00	0.29
2.02	0.50
2.98	0.59
3.91	0.74
4.97	0.84